Contributions to Geophysics and Geodesy Vol. 54/4, 2024 (301–319)

Enhancing geoid modelling for accurate local geoid determination in Lagos Island: A combined GNSS and levelling approach, Eti-Osa Local Government Area, Lagos State, Nigeria

Herbert TATA*, Olamilekan Babatunde OMODEJO

Department of Surveying and Geoinformatics, Federal University of Technology, Akure, Nigeria;
e-mails: htata@futa.edu.ng; omodejobabatunde@gmail.com

Abstract: Lagos Island faces challenges from coastal hazards and inadequate infrastructure, making precise geoid modelling essential for urban planning, flood risk assessment, and infrastructure development. This study addresses discrepancies in height references and emphasizes the need for accurate geoid data to support spatial planning and disaster management. The main objective is to create a geoid model tailored to Lagos Island's unique geography and infrastructure needs. The research combines the Global Navigation Satellite System (GNSS) and levelling data which created a reliable framework for determining geoid heights with high precision across Lagos Island. The methodology uses spirit levelling to obtain orthometric heights and GNSS technology, precisely Promak2 differential GNSS Receiver, to collect positional data. Ninety stations were surveyed to ensure comprehensive area coverage. This data was used to develop a geoid model through geometrical interpolation, accurately representing the local geoid surface. In the independent test, where 10 points were excluded from interpolation, the modelled geoid heights showed an RMSE of 0.2 metres, with the largest and smallest absolute deviations being 0.4 metres and 0.01 metres, respectively. In the non-independent test, where all points were used for interpolation, the comparison between the computed (observed) and modelled geoid heights at the same points showed a mean deviation of −0.3 metres. The RMSE and standard deviation were both 0.1 metres, confirming the model's accuracy in determining the local geoid. This demonstrates its suitability for precise local geoid determination in Lagos Island, providing a valuable tool for spatial analysis, infrastructure planning, and disaster mitigation. The study highlights the importance of integrating traditional surveying techniques with modern GNSS technology to address coastal urban challenges.

Key words: GNSS, levelling, geoid modelling, orthometric heights

*corresponding author, e-mail: htata@futa.edu.ng

doi: 10.31577/congeo.2024.54.4.1

1. Introduction

Geodesy is the "science of the measurement and mapping of the Earth's surface" (*Helmert, 1880*). This definition has to this day retained its validity; it includes the determination of the Earth's external gravity field as well as the surface of the ocean floor. With this definition, which has to be extended to include temporal variations of the Earth and its gravity field, geodesy may be included in the geosciences and also in the engineering sciences (*Helmert, 1880*).

Geodesy aims to determine the geoid, which represents the equipotential surface of the earth's gravity field and coincides with the mean sea level. The geoid is smoother than the physical surface but more irregular than the ellipsoid. It has a clear physical meaning as it can be measured over oceans, but it is not used for computations because it lacks a mathematical representation. Essentially, the geoid provides an accurate figure of the earth's shape, but its irregularity limits its use in mathematical computations (*Erol and Çelik, 2022; Deakin, 1996*).

Ellipsoidal and geodetic heights are purely geometric and lack physical meaning, making them unsuitable for practical applications in surveying, engineering, and geophysics (*Kotsakis, 2007*). Surveying equipment is typically aligned with the local gravity vector, meaning that measurements based on ellipsoidal heights cannot meet the requirements of these fields (*Featherstone et al., 1998*). Since ellipsoidal heights do not correspond to any physical reference, they must be transformed into a height system that can serve practical surveying and geodetic purposes. Without this transformation, ellipsoidal heights have limited use in real-world applications.

Determination of geoid has been one of the main research areas in the Science of Geodesy for decades. According to the widespread use of GNSS in geodetic applications, great attention is paid to the precise determination of local/regional geoid to replace the geometric levelling, which is very onerous measurement work, with GNSS surveys.

GNSS technique provides the surveyor with three-dimensional coordinates, including ellipsoidal heights (h) with respect to its reference ellipsoid, the geocentric WGS84 (World Geodetic System, 1984). As in GNSS measurements, geodesists have chosen an oblate ellipsoid of revolution, flattened at the poles, to approximate the geoid to simplify survey data reduction and mapping.

However, most surveying measurements are made in relation to the geoid, which is the equipotential surface of the earth's gravity field, not ellipsoid because the equipment is aligned with the local gravity vector, which is perpendicular to the geoid surface, usually through the use of a spirit bubble (*Featherstone et al., 1998*). Because of these facts, ellipsoidal heights can't satisfy the aims in practical surveying, engineering or geophysical applications as they have no physical meaning and must be transformed to orthometric heights (H), which are referred to as geoid, to serve the geodetic and surveying applications. To accomplish this transformation between ellipsoidal heights and orthometric heights, it is necessary to determine their undulation (N). A WGS84 ellipsoidal height (h) is transformed into an orthometric height (H) by subtracting the geoid-WGS84-ellipsoid separation (N), called geoid undulation. Depending on data availability and accuracy requirements, there are two principal approaches for determining geoid models, which are utilised to transform GNSS ellipsoidal heights to orthometric heights. These approaches include a gravimetric method and interpolation between geometrically derived geoid heights using the benchmarks of which three-dimensional coordinates and orthometric heights have been determined according to GNSS and levelling measurements.

This study focuses on the geoid modelling technique based on the geometrical interpolation approach by fitting a surface that depends on the reference points that will be chosen in the critical and characteristic locations of the field to represent the trend of the geoid surface. Empirical geoidal undulations for all points will be computed using the orthometric heights and the ellipsoidal heights. A multiple regression model will also be formulated in this project work as the required geometrical model to adjust the derived geoid adjust the derived geoid further, adjust the derived undulations further adjust the derived geoid undulations using a surface interpolation (kriging) approach, the coordinate and the computed geoidal heights of some well-selected points will be utilised gridding. This will be used as a model for generating the geoidal heights of any other arbitrary points whose coordinates are known.

1.1. Geoid modelling

There are different methods for modelling geoid, either local or global models derived as part of a global or regional geodetic infrastructure. Globally, the

determination of the geoid has been carried out by various researchers. Different geoid modelling techniques have been detailed in *Alem et al. (2016), Nwilo et al. (2012), Atomode (2019), Featherstone and Sproule (2006), Tata and Ono (2018), Raufu and Tata (2022), Tata and Okiemute (2021), Kiamehr and Sjöberg (2005), Idowu et al. (2014), Fotopoulos (2003), Denker et al. (2009), Deakin (1996), Erol and Çelik (2022), Dayoub et al. (2012), Jekeli and Garcia (2006), Moka et al. (2006), Hirt and Bürki (2006).*

1.2. Study area

The study area (Figure 1a) is Lagos Island Local Government Area, in Lagos State, South-Western, Nigeria which is located at $6^\circ\,30'\,0''$ N – $6^\circ\,45'\,0''$ N, $3^\circ\,30'\,0''$ E – $3^\circ\,45'\,0''$ E. It falls within an area of 9 sq. kilometres approximately with a perimeter of about 11.52 Lagos Island Local Government Area is regarded as a disparate settlement because the area serves as both a commercial centre and a residential area. The areas that formed the Local Government include Adeniji Adele, Obalende, CMS, Marina district, etc (*Dauda, 2007*). Figure 1b shows a 2D map of the study area indicating the spatial distribution of specific points or stations where data collection or observations were made. The red dots on the map represent the locations of the stations used in the study. Each station is marked with a unique identifier (e.g., A1, A2, A3, etc.) and the stations are spread across the entire study area.

2. Methods

The data utilized for the research were acquired from both primary and secondary sources. In this study, these include orthometric heights which were obtained from spirit levelling as well as ellipsoidal height using the Global Positioning System (GNSS), several common points (benchmarks) were observed using both GNSS and levelling. The GNSS was used in rapid static differential mode for five minutes per station. The coordinate of the control point was collected from the Surveyor General office in Alausa, Lagos. Geoid heights of the observed stations were obtained from both ellipsoidal heights from the GNSS observations and orthometric heights from the levelling of each observed station.

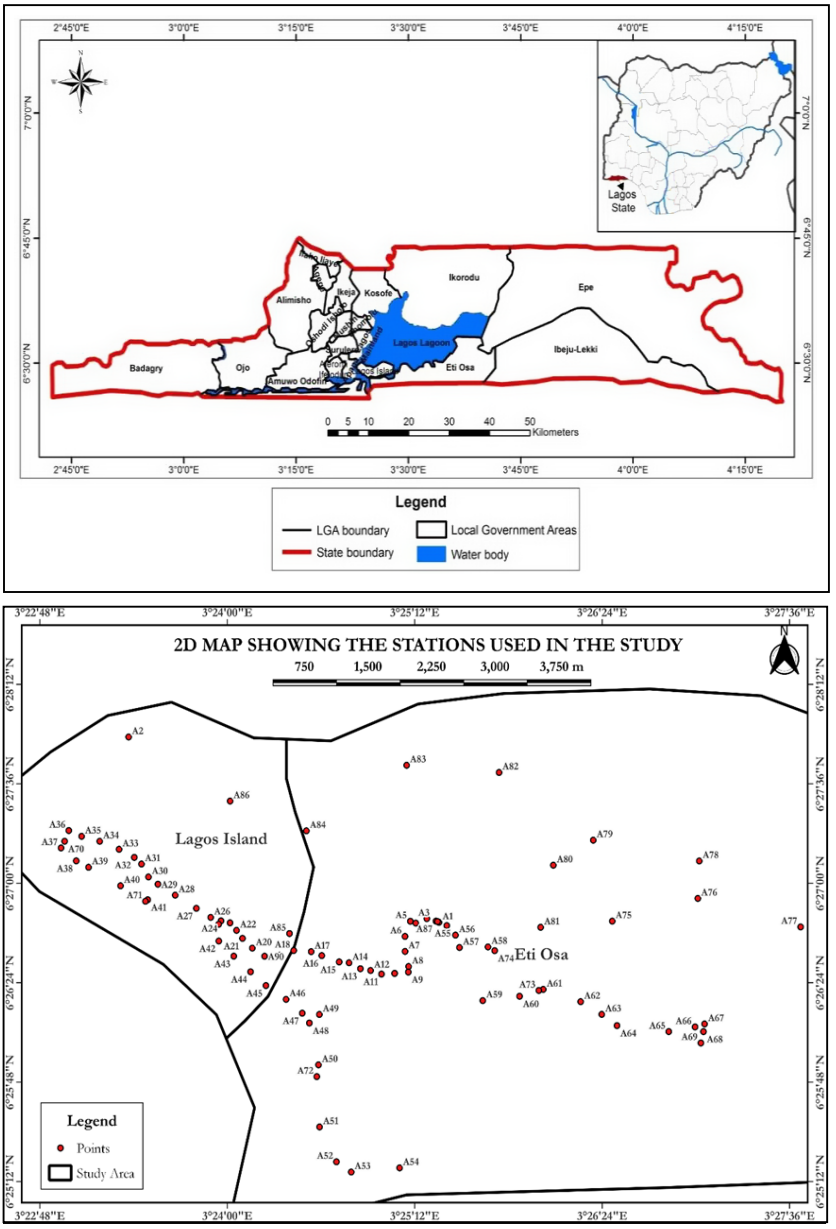

Fig. 1. Map of the study area (a), source: *Atomode (2019)*; (b) showing a 2D map of the study area.

Therefore, 5-a parameter transformation model was used in developing a local geoid model for the area of study. The coefficient of the transformation model was computed using least square techniques. The computed geoid height and modelled geoid height were compared to evaluate the performance of the model. The developed model was used to build a computational tool for determining local geoid over the study area. This computational tool is developed to compute the geoid height and also the orthometric height of observed points within the area of study.

2.1. GNSS observation procedures

This is the core of the methodology where all possible data are gathered systematically according to the pre-arranged scheme. Here we carried out the kinematic GNSS positioning following the rules from the succeeding stage. The nitty-gritty of the steps taken during data acquisition is outlined below.

2.1.1. Base station occupation

The first step of the GNSS observation was to occupy the master station. This was done with the steps of orientation (i.e. placing the tri-bach on the tripod, centring the tripod on the nob of the control beacon with the optical plummet, ensuring the stability of the tripod around the beacon and finally levelling the instrument on the tripod. This is done after fixing the master receiver on the tri-bach, and then making sure it is horizontally levelled by using the tri-bach skews to adjust the spirit level).

Thereafter, the necessary connection was made:

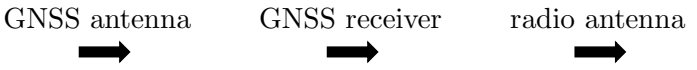

2.2. Levelling data deduction

The collimation method, also known as the height of instrument (HI) method, was used to determine the orthometric heights of various points relative to a known benchmark. For this operation to be performed, a two-peg test must be carried out to determine if the quality and accuracy of the instrument meet the standard for the operation Table 1. In this research,

the operation was carried out in closed-loop levelling nets in order to obtain the height differences between the points.

To begin, the levelling instrument was set up between the benchmark and the points to be measured. A backsight reading was taken on a levelling staff placed on the benchmark, and this reading was added to the benchmark's known elevation to calculate the height of the instrument – Eq. (1). Subsequent, foresight readings were taken at the points where the elevation was to be determined. The elevation of each point is then found by subtracting the foresight reading from the height of the instrument – Eq. (2). This process was repeated for multiple points, and if the instrument needed to be moved, the last foresight reading became the backsight reading for the new setup.

It is very important to carry out checks on the observed backsight, foresight and computed reduced-level readings. These checks will assist the observer in detecting possible gross errors as well as misclosure. For this research, checks were carried out at each loop using Eq. (3).

This Reduced level (RL) is the height of a point relative to a specific reference plane, typically mean sea level or a benchmark. The term "reduced" indicates that the elevation has been adjusted relative to this common datum, allowing for consistent comparisons across different locations.

Table 1. Two-peg test computation.

setup	**back sight (mm)**	**foresight (mm)**	**difference (mm)**
1st setup true height difference	1.554	1.552	0.001
2nd setup apparent difference	1.560	1.558	0.002
error difference			0.001

The collimation error for the two-peg test was found to be 0.001 mm and 0.002 mm, indicating that the instrument is in good order and can be used to carry out observations.

$$\mathrm{HC} = \mathrm{RL} + \mathrm{BS}\,, \tag{1}$$

$$\mathrm{RL} = \mathrm{HC} - \mathrm{FS/IS}\,, \tag{2}$$

$$\text{Check:}\ \sum \mathrm{BS} - \sum \mathrm{FS} = \text{first RL} - \text{last RL}\,, \tag{3}$$

where BS = backsight, FS = foresight, IS = intermediate sight, RL = reduced level and HC = height of collimation.

2.3. Geoid height (*N*) computation

GNSS/Leveling geoid of the observed point was computed from Eq. (1) as stated below:

$$N^{NGNSS/Lev} = h - H\,, \tag{4}$$

where H and h are the orthometric and ellipsoidal height of points, respectively.

The former was obtained from the levelling operation, while the latter was obtained from the GNSS observation. This computation was done using Microsoft Excel.

2.4. Local geoid modelling

In modelling the local geoid of the study area, the 5-parameter transformation model used by *Fotopoulos (2003)* was adopted. The expression is given in Eq. (5).

The 5-parameter transformation model with model coefficients x_i can be expressed as:

$$N(X,Y) = x_1 + x_2\,\cos Y_i\,\cos X_i + x_3\,\cos Y_i\,\sin X_i + x_4\,\sin Y_i + \\ + x_5\,\sin^2 Y_i\,, \tag{5}$$

coefficients of transformation: N = geoidal heights, (X,Y) = easting and northing coordinates.

In this research work, there are ninety (90) control points which were uniformly distributed within the area of study. These points have their precise horizontal and vertical locations with respect to easting (x) and northing (y), the ellipsoidal heights (h) and the orthometric height (H).

The 5-parameter transformation models in Eq. (5) are defined by using the geoidal separation 'N' and the horizontal coordinates x, and y of the control points. Considering the polynomial in Eq. (5), at least with ninety control points whose N, x, y is known, the coefficients from x_1 to x_5 were computed thus defining the exact mathematical relation. Thereafter, this model was used to obtain the N value for any location by inserting the horizontal coordinates x and y.

In this study, ninety control points whose geoidal undulation, easting and northing coordinates were used in computing the model coefficients of the 5-parameter transformation model (Eq. (5)) using least square techniques.

2.5. Least squares adjustment technique

The computation of the polynomial coefficients was done by the observation equation method of the least square adjustment technique. The observation equation of least square observation was presented by matrix notation as given by *Ono et al. (2018)*:

$$V = A\,x - L\,, \tag{6}$$

$$x = (A^T A)^{-1} A^T L\,, \tag{7}$$

where A = design matrix, x = vector of unknowns, L = observation matrix, and V = residual matrix.

2.6. Formation of matrix $\boldsymbol{A}$

Matrix A was formed by partial derivatives of the coefficients a_i as regards (X, Y). Matrix A is the matrix of the coefficient of the unknowns. The dimension for A matrix is ${}_{\boldsymbol{m}}\boldsymbol{A}^{\boldsymbol{n}}$ which is the number of observations (m) by the number of unknowns (n). So, when forming matrix, A, one must first determine the actual number of observations and unknown parameters. The number of unknown parameters formed the column of matrix A, while the number of observations forms the row of matrix A.

Matrix A was formed for the 5-parameter transformation model. It is expressed as:

$$A_{m\times 93} = \begin{bmatrix} 1 & \cos\varphi_i \cos\lambda_i & \cos\varphi_i \sin\lambda_i & \sin\varphi_i & \sin^2\varphi_i \\ \vdots & \vdots & \vdots & \vdots & \vdots \\ 1 & \cos\varphi_{m-1} \cos\lambda_{m-1} & \cos\varphi_{m-1} \sin\lambda_{m-1} & \sin\varphi_{m-1} & \sin^2\varphi_{m-1} \\ 1 & \cos\varphi_m \cos\lambda_m & \cos\varphi_m \sin\lambda_m & \sin\varphi_m & \sin^2\varphi_m \end{bmatrix}.$$

2.7. Formation of matrix $\boldsymbol{L}$

Matrix L is the matrix of observations. It has a dimension of ${}_{\boldsymbol{m}}\boldsymbol{L}^{\boldsymbol{1}}$, where m is the number of observations. For this study, we have a matrix of $90\times\mathbf{1}$

for the observation matrix, which means we will have ninety (90) rows and one (1) column. Observation matrix L is the ΔN value for each station. N was calculated using Eq. (4). The matrix L is expressed as follows:

$$L_{m\times 1} = \begin{bmatrix} N(X_i, Y_i) \\ N(X_{i+1}, Y_{i+1}) \\ \vdots \\ N(X_{m-1}, Y_{m-1}) \\ N(X_m, Y_m) \end{bmatrix}. \tag{8}$$

2.8. Vector of unknowns/model parameter x

Since matrices A and L have been formed, the vector of unknowns/model parameter x was computed using Eq. (7):

$$x = (A^T A)^{-1} A^T L\,.$$

The vector of unknowns/model parameter x was computed for the 5-parameter transformation model using this Eq. (5).

2.8.1. Vector of residuals V

Matrix V is the matrix of residual. It has a dimension of $\boldsymbol{_m V^1}$ where 'm' is the number of observations. Therefore, the vector of residual is computed for the transformation models by using Eq. (6).

MATLAB program was written to compute the vector of unknowns/model parameter x and the vector of residual V.

Aposterior variance was computed using the formula:

$$\text{Aposterior variance} = \sqrt{\frac{V^T V}{m-n}}\,, \tag{9}$$

where m = number of observations, n = number of parameters.

2.9. Assessment of the model performance

The performance of the developed model from the 5-parameter transformation model used in modelling the local geoid of the study area was assessed by using the coordinates of some observed stations to compute the geoidal height of the same points. Therefore, the geoid height computed

from the model was compared with the observed computed geoid height. Performance measures like root mean square error (RMSE) and standard deviation were used in this study for performance assessment of the local geoid model for the study area.

The average RMSE calculated in this way offers a more accurate picture of the performance of the local geoid model selected as a prediction surface for a new point. Root mean square error and standard deviation were computed using Eq. (10):

$$\mathrm{RMSE} = \sqrt{\frac{\sum_{i=1}^{n} (y_i - x_i)}{n}}\,. \tag{10}$$

3. Results and discussion

3.1. Ellipsoidal and orthometric heights

Results of the ellipsoidal and orthometric heights for the observed stations are shown in Table 2. The table consists of results for the northing and easting coordinates, ellipsoidal height, and computed orthometric height of each observed station.

3.1.1. Validation of geoid model

Table 3 shows ten (10) points excluded from the total ninety (90) points observed for the study used to independently validate the performance of a geoid model by comparing its predictions (modelled heights) with actual measurements (computed heights). In Table 4, the computed geoid height represents the actual geoid height that was computed at each station. The modelled geoid height is the predicted geoid model at each station while the difference is between the computed geoid height and the modelled geoid height for each station. The difference values show how closely the modelled geoid height fits the computed geoid height at each station. Positive values indicate that the model predicted a lower height than was computed, while negative values indicate the opposite. MSE and RMSE provide overall measures of how well the model performs across all stations. Lower values indicate a better fit. Aposterior variance reflects the variability of the model's errors after adjusting for the data, which was useful in understanding the reliability of the model's predictions.

Table 2: Result of ellipsoidal and orthometric heights (sample data extracted from the complete data).

station codes	**easting (mE)**	**northing (mN)**	**ellipsoidal heights (m)**	**orthometric heights (m)**
A1	546728.547	712534.687	0.998	1.216
A2	543064.991	714592.260	0.945	1.236
A3	546584.191	712575.344	1.184	1.225
A4	546454.116	712525.569	0.936	1.303
A5	546389.977	712546.083	0.939	1.315
A6	546327.234	712377.094	1.114	0.908
A7	546328.260	712211.135	0.366	0.215
A8	546370.269	712043.095	−0.327	−0.059
A9	546366.513	711981.195	−0.356	−0.043
A10	546205.795	711967.274	−0.217	−0.002
A11	546050.028	711958.468	−0.263	−0.128
A12	545921.508	711998.202	−0.648	−0.360
A13	545801.161	712018.163	−0.649	−0.427
A14	545667.78	712084.133	−0.600	−0.452
A15	545551.059	712093.195	−0.595	−0.325
A16	545345.473	712163.113	−0.244	0.115
A17	545220.466	712207.210	−0.084	0.220
A18	545014.456	712219.580	−0.186	0.112
A19	544847.851	712167.669	−0.045	0.225

Table 3. Showing validation of the geoid model.

station	**computed geoid height(m)**	**modelled geoid height(m)**	**difference (m)**
A1	−0.22	−0.24	0.02
A2	−0.29	−0.28	−0.01
A3	−0.04	−0.28	0.24
A4	−0.37	−0.26	−0.11
A5	−0.38	−0.22	−0.15
A6	0.21	−0.23	0.43
A7	0.15	−0.27	0.42
A8	−0.27	−0.23	−0.04
A9	−0.31	−0.23	−0.08
A10	−0.22	−0.25	0.03
MSE			**0.05**
RMSE			**0.22**
Aposterior variance			**0.18**

3.1.2. Computed geoid heights result

The results of computed geoid heights for some of the observed stations are shown in Table 4.

Table 4. Result of computed geoid heights (sample data extracted from the complete data of 90 points).

station codes	easting (mE)	northing (mN)	computed geoid height (m)
A1	546728.547	712534.687	−0.218
A2	543064.991	714592.260	−0.291
A3	546584.191	712575.344	−0.041
A4	546454.116	712525.569	−0.367
A5	546389.977	712546.083	−0.376
A6	546327.234	712377.094	0.206
A7	546328.260	712211.135	0.151
A8	546370.269	712043.095	−0.268
A9	546366.513	711981.195	−0.313
A10	546205.795	711967.274	−0.215
A11	546050.028	711958.468	−0.135
A12	545921.508	711998.202	−0.288
A13	545801.161	712018.163	−0.222
A14	545667.780	712084.133	−0.148
A15	545551.059	712093.195	−0.270
A16	545345.473	712163.113	−0.359
A17	545220.466	712207.210	−0.304
A18	545014.456	712219.580	−0.298
A19	544847.851	712167.669	−0.270

3.1.3. Computed vector for unknown parameters (x)

The result of the vector for unknown parameters (x), which was the coefficient of the 5-parameter transformation model as given by MATLAB is presented in Table 5.

The 5-parameter transformation models in Eq. (5) of the local geoid model can be expressed as:

$$N(\varphi,\lambda)N(\varphi,\lambda) = -0.2633 + 0.0102\,\cos\varphi_i \cos\lambda_i - 0.0017\,\cos\varphi_i \sin\lambda_i + \\ + 0.0268\,\sin\varphi_i + 0.0137\,\sin^2\varphi_i\,.$$

Table 5. Result of vector of unknown parameters for 5-parameter transformation model.

5-parameter transformation model	
coefficient	**values**
a_0	−0.2633
a_1	0.0102
a_2	−0.0017
a_3	0.0268
a_4	0.0137

3.1.4. Differences between computed geoid height and modelled geoid height results

The comparison of computed geoid height and the model geoid height computed from a developed model for 90 stations is summarized in Table 6.

Table 6. Differences between the computed geoid height and model geoid height computed from the developed model.

station	**geoid height (N)**	**modelled geoid height (devN)**	**diff. in geoid height (N−devN)**
A1	−0.22	−0.27	0.06
A2	−0.29	−0.38	0.09
A3	−0.04	−0.28	0.23
A4	−0.37	−0.28	−0.09
A5	−0.38	−0.28	−0.10
A6	0.21	−0.28	0.48
A7	0.15	−0.28	0.43
A8	−0.27	−0.27	0.01
A9	−0.31	−0.27	−0.04
A10	−0.22	−0.27	0.06
A11	−0.14	−0.27	0.14
A12	−0.29	−0.27	−0.02
A13	−0.22	−0.27	0.05
A14	−0.15	−0.27	0.12
A15	−0.27	−0.27	0.00
A16	−0.36	−0.27	−0.09
A17	−0.30	−0.27	−0.04
A18	−0.30	−0.26	−0.03
A19	−0.27	−0.26	−0.01

The graphical representation of computed geoid height and modelled geoid height of observed points are described in Fig. 2. The computed geoid

height is shown in the blue line while the modelled geoid height is represented in orange colour. The modelled geoid height showed little variation at some points while there is a large variation at some points which can be a result of variation in terrain which is not accounted for in the model. However, the modelled geoid height still shows the approximate representation of the true nature of the terrain of the study area and it can be adopted for local geoid modelling within the study area.

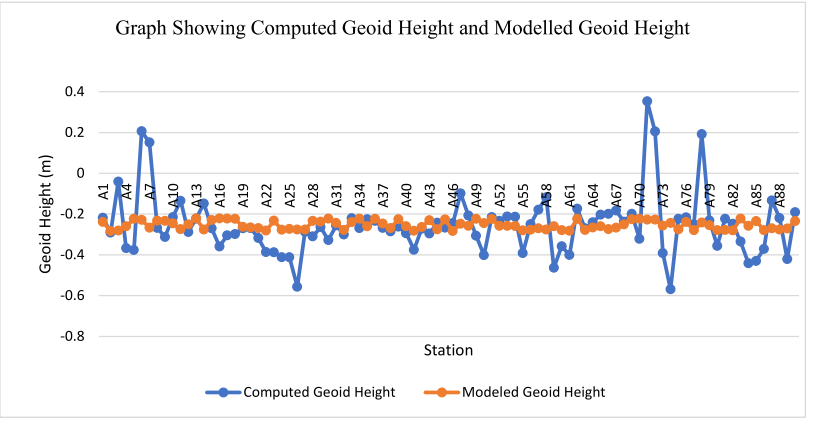

Fig. 2. Graphical representation of the computed and modelled geoid heights.

Figures 3 and 4 show the contour maps of the computed geoid height and modelled geoid height, respectively. Surfer 10 software was used to plot the contour map, kriging gridding method was applied at 0.003 m and 0.06 contour intervals. The contour maps have the same patterns which indicate that both (computed geoid height and modelled geoid height) are the true representation of the terrain. The surface model for the modelled geoid height approximately follows the same slope as the surface model for the computed geoid height which indicates that both are natural height systems.

3.2. Analysis of results

The statistics of the computed geoid height and modelled geoid height are summarized in Table 7 in terms of maximum deviation (max.), minimum deviation (min.) and mean deviation (mean).

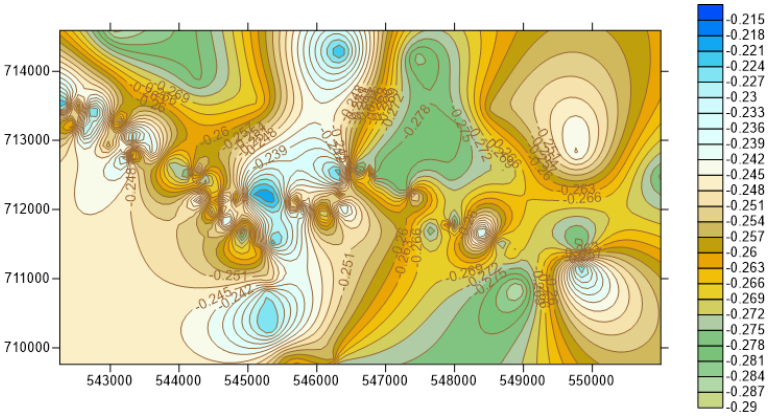

Fig. 3. Contour map of the computed geoid height.

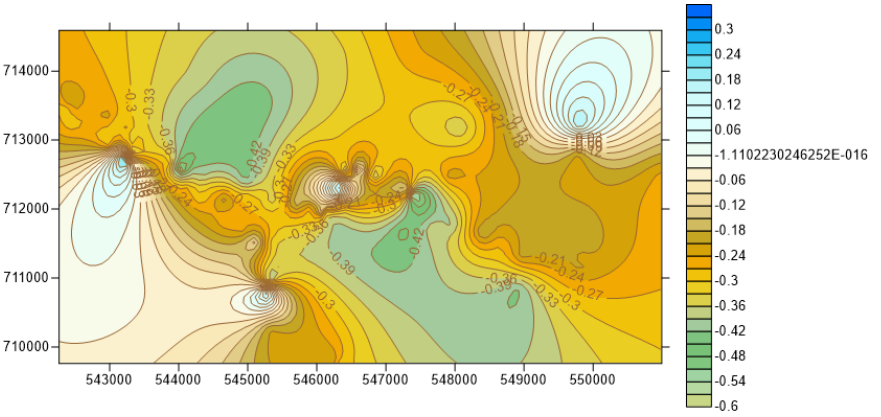

Fig. 4: Contour map of the modelled geoid height.

Table 7 shows the maximum deviation for the computed geoid height and modelled geoid height is 0.35 m and 0.22 m respectively with the modelled geoid height having the least maximum deviation value. The computed geoid height also has the least minimum deviation value of −0.28 m when compared with that of the modelled geoid height with a value of −0.57 m. The mean deviation for computed geoid height and modelled geoid height is −0.25 m and −0.25 m, respectively. The modelled geoid height also has the same mean deviation value although the difference in their value is minor and not significant.

Table 7. Statistics of the computed geoid height and modelled geoid height.

statistics	computed geoid height (N) m	modelled geoid height (devN) m
max.	0.35	0.22
min.	−0.57	−0.28
mean	−0.25	−0.25

4. Conclusion

In this research, a local geoid model was developed for local geoid determination in the study area using GNSS and levelling data from 90 stations. GNSS and levelling data were processed to get the northing, easting, ellipsoidal height and orthometric height of observed stations. Therefore, the geoid height of observed stations was obtained from the difference between ellipsoidal height and orthometric height of each observed station.

The 5-parameter transformation model was used in developing a local geoid model for the study. The coefficient of the transformation model was computed using least square techniques. The aposterior variance was 0.1899 m. Geoid heights were computed from this model and the values were compared with the computed geoid height.

The study compared the computed and modelled geoid heights in a study area. The computed geoid height had the least maximum deviation of 0.35 m and minimum deviation of −0.57 m, while the modelled geoid height had the least maximum deviation of 0.22 m and minimum deviation of −0.28 m. The modelled geoid height showed some variation, possibly due to terrain variations. However, it accurately represents the true terrain of the study area and can be used for local geoid modelling within the study area. The model's standard deviation and root mean square error were calculated, and it can be used to compute geoid heights at any point in the area. The local geoid model developed in this research is hereby recommended for accurate local geoid determination in the study. Furthermore, the developed computational tool is recommended for computing geoid height and also orthometric height of points within the area of study.

Acknowledgements. The research was self-sponsored.

Declaration of competing interest. The authors declare that there are no competing interests.

Authors' contributions. Conceptualization: T. H.; Data curation: T. H., O. B.; Formal analysis: O. B.; Funding acquisition: O. B.; Investigation: T. H., O. B.; Methodology: T. H., O. B.; Project administration: T. H., O. B.; Resources: O. B.; Software: O. B.; Supervision: T. H.; Validation: T. H.; Visualization: T. H., O. B.; Roles/ Writing – original draft: T. H., O. B.; Writing – review and editing: T. H., O. B.

References

Aleem K. F., Adesoye A. A., Bankole A. L., 2016: Practical Determination of Geoidal Undulation and Geoidal Map of Part of Mubi, Adamawa State, Nigeria. Int. J. Eng. Res. Technol., **5**, 4, IJERTV5IS041031, 740–747.

Atomode I. T., 2019: Spatial Pattern of Urban Freight Traffic Problems in Lagos State, Nigeria. J. Res. Dev. Arts Soc. Sci., **5**, 248–269.

Dauda S. O., 2007: Development of an Automated Geoid Model (Unpublished). B.Sc Project Report, Department of Surveying and Geoinformatics, University of Lagos, Akoka, Nigeria.

Dayoub N., Edwards S. J., Moore P., 2012: The Gauss–Listing geopotential value W_0 and its rate from altimetric mean sea level and GRACE. J. Geod., **86**, 9, 681–694, doi: 10.1007/s00190-012-0547-6.

Deakin R. E., 1996: The Geoid what's it got to do with me? Aust. Surv., **41**, 4, 294–305, doi: 10.1080/00050339.1996.10558646.

Denker H., Barriot J.-P., Barzaghi R., Fairhead D., Forsberg R., Ihde J., Kenyeres A., Marti U., Sarrailh M., Tziavos I. N., 2009: The development of the European Gravimetric Geoid model EGG07. In: Sideris M. G. (Ed.): Observing our Changing Earth. International Association of Geodesy Symposia, **133**, pp. 177–185, Springer, Berlin, Heidelberg, doi: 10.1007/978-3-540-85426-5_21.

Erol B., Çelik R. N., 2022: Precise determination of geoid models with an aim to replace the geometric levelling measurements with GNSS measurements during geodetic and surveying works. ITU, Civil Engineering Faculty, Geodesy Division, 34469 Maslak Istanbul.

Featherstone W. E., Evans J. D., Olliver J. G., 1998: A Meissl-modified Vaníček and Kleusberg kernel to reduce the truncation error in gravimetric geoid computations. J. Geod., **72**, 3, 154–160, doi: 10.1007/s001900050157.

Featherstone W. E., Sproule D. M., 2006: Fitting AUSGeoid98 to the Australian height datum using GPS-levelling and least squares collocation: Application of a cross-validation technique. Surv. Rev., **38**, 301, 573–582, doi: 10.1179/sre.2006.38.301.573.

Fotopoulos G., 2003: An analysis of the optimal combination of geoid, orthometric and ellipsoidal height data. PhD thesis, report No. 20185, University of Calgary, Calgary.

Helmert F. R., 1880: Die mathematischen und physikalischen theorieen der höheren geodäsie; Einleitung und 1. Teil: Die mathematischen Theorieen (The mathematical and physical theories of higher geodesy; Introduction and Part 1: The mathematical theories). Leipzig, B. G. Teubner, 1241 p. (in German).

Hirt C., Bürki B., 2006: Status of geodetic astronomy at the beginning of the 21st century, Festschrift Univ.-Prof. Dr. – Ing. Prof. h.c. Günter Seeber anlässlich seines 65. Geburtstages und der Verabschiedung in den Ruhestand. In: Hirt C. (Ed.): Wissenschaftliche Arbeiten der Fachrichtung Geodäsie und Geoinformatik an der Universität Hannover, **258**, 81–99, University of Hannover.

Idowu T. O., Edan J. D., Abubakar T., Aliyu M. R., 2014: Determination of orthometric heights from GNSS and levelling data. Department of Surveying and Geoinformatics, Federal University of Technology Akure, Nigeria.

Jekeli C., Garcia R., 2006: Local geoid determination with in situ geopotential data obtained from satellite-to-satellite tracking. In: Sideris M. G. (Ed.): Gravity, Geoid, and Geodynamics 2000, Proceedings of International Association of Geodesy Symposia, **123**, pp. 123–128, Springer-Verlag, Berlin, doi: 10.1007/978-3-662-04827-6_20.

Kiamehr R, Sjöberg L. E., 2005: Comparison of the qualities of recent global and local gravimetric geoid models in Iran. Stud. Geophys. Geod., **49**, 3, 289–304, doi: 10.1007/s11200-005-0011-7.

Kotsakis C., 2007: Transforming ellipsoidal heights and geoid undulations between different geodetic reference frames. J. Geod., **82**, 4-5, 249–260, doi: 10.1007/s00190-007-0174-9.

Moka E. C., Agajelu S. I., Okeke F. I., 2006: An Assessment of the Distortions in a Part (K-Chain) of the Nigerian Horizontal Geodetic Network. General Assembly Conference of the Nigeria Association of Geodesy, Lagos, 23-25 August 2006, 15–29.

Nwilo P. C., Opaluwa Y. D., Adejare Q. A., Ayodele E. G., Ayeni A. M., 2012: Geoid modelling using geometrical interpolation technique. Department of Surveying and Geoinformatics, University of Lagos, Akoka – Yaba, Lagos State, Nigeria.

Ono M. N., Eteje S. O., Oduyebo F. O., 2018: Comparative Analysis of DGPS and Total Station Accuracies for Static Deformation Monitoring of Engineering Structures. IOSR J. Environ. Sci. Toxicol. Food Technol. (IOSR-JESTFT), **12**, 6, 19–29, doi: 10.9790/2402-1206011929.

Raufu I. O., Tata H., 2022: Comparison of Two Corrector Surface Models of Orthometric Heights from GNSS/Levelling Observations and Global Gravity Model. J. Geospat. Inf. Sci. Eng. (JGISE), **5**, 1, 15–20, doi: 10.22146/jgise.72531.

Tata H., Okiemute E. S., 2021: Determination of Orthometric Heights of Points Using Gravimetric/GNSS and Geodetic Levelling Approaches. Indian J. Eng., **18**, 49, 134–144.

Tata H., Ono M. N., 2018: A Gravimetric Approach for the Determination of Orthometric heights in Akure Environs, Ondo State, Nigeria. J. Environ. Earth Sci., **8**, 8, 75–80, doi: 10.7176/JEES/8-8-07.